


Earthquake hazard and risk assessment based on Unified Scaling Law for Earthquakes: Greater Caucasus and Crimea

Vladimir G. Kossobokov · Anastasia K. Nekrasova 

Received: 13 March 2018 / Accepted: 10 May 2018 / Published online: 24 May 2018
© Springer Science+Business Media B.V., part of Springer Nature 2018

Abstract We continue applying the general concept of seismic risk analysis in a number of seismic regions worldwide by constructing regional seismic hazard maps based on morphostructural analysis, pattern recognition, and the Unified Scaling Law for Earthquakes (USLE), which generalizes the Gutenberg-Richter relationship making use of naturally fractal distribution of earthquake sources of different size in a seismic region. The USLE stands for an empirical relationship $\log_{10}N(M, L) = A + B \cdot (5 - M) + C \cdot \log_{10}L$, where $N(M, L)$ is the expected annual number of earthquakes of a certain magnitude M within a seismically prone area of linear dimension L . We use parameters A , B , and C of USLE to estimate, first, the expected maximum magnitude in a time interval at seismically prone nodes of the morphostructural scheme of the region under study, then map the corresponding expected ground shaking parameters (e.g., peak ground acceleration, PGA, or macro-seismic intensity). After a

rigorous verification against the available seismic evidences in the past (usually, the observed instrumental PGA or the historically reported macro-seismic intensity), such a seismic hazard map is used to generate maps of specific earthquake risks for population, cities, and infrastructures (e.g., those based on census of population, buildings inventory). The methodology of seismic hazard and risk assessment is illustrated by application to the territory of Greater Caucasus and Crimea.

Keywords Unified Scaling Law for Earthquakes · Earthquake hazard · Seismic risk · Morphostructural zoning · Earthquake prone node · Maximum credible magnitude

1 Introduction

Seismic reality evidences many contradictions to the model assumption of a stationary Poisson point process. Eventually, a response to these leads to complications of the existing hypotheses by introducing sequences of main events and their associates (fore- and after-shocks) superimposed with hypothetical distributions of the associate size, time, and location. Therefore, among other fundamental shortcomings related with inadequate characterization of ground shaking, estimation of the annual rate of magnitude M earthquakes, $N(M)$, at a given site of interest remains the basic source of erroneous seismic hazard assessment (Kossobokov and Nekrasova 2012; Panza et al. 2014; Nekrasova et al. 2014; Kossobokov

V. G. Kossobokov (✉) · A. K. Nekrasova (✉)
Institute of Earthquake Prediction Theory & Mathematical
Geophysics, RAS, Moscow, Russian Federation
e-mail: volodya@mitp.ru
e-mail: nastia@mitp.ru

V. G. Kossobokov
Geophysical Center, RAS, Moscow, Russian Federation

V. G. Kossobokov
Institut de Physique du Globe de Paris, Paris, France

V. G. Kossobokov
International Seismic Safety Organization, Arsita, Italy

et al. 2015), contributing to disastrous seismic engineering decisions (Davis et al. 2012).

The results of the global and regional analyses (Kossobokov and Mazhkenov 1994; Nekrasova and Kossobokov 2002, 2005, 2006, 2016; Kossobokov 2005; Nekrasova 2008; Nekrasova et al. 2011, 2015; Parvez et al. 2014) imply that the occurrence of earthquakes at a seismically prone site x , for a wide range of magnitudes $M \in (M_-, M_+)$ and sizes $L \in (L_-, L_+)$, can be described by the following formula:

$$N(M, L) = 10^A \times 10^{B \times (5-M)} \times L^C \quad (1)$$

where $L \times L$ is a square embedding seismic locus and A , B , and C are constants. An alternative formulation using the inter-event time instead of rate of occurrence has been suggested by Bak et al. (2002) as Unified Scaling Law for Earthquakes (USLE). The name introduced in (Bak et al. 2002; Christensen et al. 2002) applies to the generalization of Gutenberg-Richter relationship by Kossobokov and Mazhkenov (1994) given in the following form:

$$\log_{10} N(M, L) = A + B \times (5-M) + C \times \log_{10} L \quad (2)$$

where $N(M, L)$ is the expected annual number of earthquakes of a certain magnitude M within a seismically prone area of diameter L , A , and B characterize the annual rate of magnitude 5 events and the balance between magnitude ranges, correspondingly (analogous to a - and b -values of Gutenberg-Richter relationship), and C estimates the fractal dimension of the epicenter support.

Note that (1) the traditional estimations of seismic hazard for cities and urban agglomerations are usually underestimated when rescaling earthquake rate of occurrence from a larger surrounding territory (Kossobokov and Mazhkenov 1994; Nekrasova et al. 2015) with non-uniform distribution of earthquake sources (Beauval et al. 2006) and (2) a discrepancy in evaluation of seismic hazard propagates non-linearly into erroneous estimations of risks (Wyss et al. 2012). In a pilot application to the territory of Greater Caucasus and Crimea, we follow the methodology described below.

2 Methodology

In assessment of seismic hazard, we use an alternative to traditional methodologies. It is based on USLE and requires reliable estimation of the scaling properties of the earthquake sequences at the territory of concern. We keep applying the same methodology of seismic risks estimation as the one thoroughly described in (Parvez et al. 2014; Panza et al. 2014; Nekrasova et al. 2015; Parvez et al., 2018).

A space-time-magnitude volume, $S \times T \times M$ is considered, where S is the territory, T is time interval from T_0 to T_1 , and M is the magnitude range above M_0 ; the events with magnitude $m \geq M_0$ are reasonably complete in the catalogue since T_0 . The algorithm for Scaling Coefficients Estimation, named SCE (Nekrasova et al. 2015), applies to a catalogue of earthquakes as the initial input data source.

In assessment of seismic hazard based on USLE, the coefficients A , B , and C defined in application of the SCE algorithm at grid points are used to determine the expected magnitude of maximum credible earthquake (MCE) events. Specifically, at the scale of tens of kilometers, the $0.25^\circ \times 0.25^\circ$ cells are set at the grid points predetermined by the nodes of morphostructural zoning (Gorshkov et al. 2003) and/or the empirical distribution of epicenters, or even some regular mash. For each $0.25^\circ \times 0.25^\circ$ cell centered at a grid point, we calculate the expected numbers of events from magnitude ranges M_j in 50 years, i.e., $N_{50}(M_j, 0.25^\circ) = 50 \times N(M_j, 0.25^\circ)$, then find the maximum magnitude (M_{\max}), with the expected number $N_{50}(M_{\max}, 0.25^\circ) \geq 10\%$. Such a determination of M_{\max} implies expectation of one MCE event in 500 years and complies with a traditional probabilistic seismic hazard analysis (PSHA) “10% chance of exceedance in 50 years” in a cell. At this step, we assess seismic hazard potential in the distributed sources of earthquake occurrence. Note that by applying an empirical estimate of mathematical expectation, we avoid the model assumption of a stationary Poisson point process in favor of a stochastic repeatability of seismic regime.

In the next step, we expand hazard assessment from the distributed earthquake sources to the entire territory of a study and convert the expected maximum magnitude M_{\max} to a characteristic of macro-seismic effect by applying the empirical formulae. For example, when considering the peak ground acceleration, PGA, we apply, at each point of a regular grid, the empirical

formula for acceleration produced by a source of M_{\max} at the irregular grid as inspired from the scenario-based neo-deterministic seismic hazard assessment study by Parvez et al. (2003), i.e.,

$$\text{Acc}(M_{\max}, D) = \text{const} \times g \times D^{-1.5} \times \exp.(M_{\max}-5) \quad (3)$$

where D is the source-receiver distance on a $0.25^\circ \times 0.25^\circ$ grid, $\text{const} = 6 \times 4.8$, $g = 9.81 \text{ m/s}^2$ is the gravity constant, and $\exp(X)$ is the natural exponent of X . The maximum of acceleration values computed at a grid point is assigned to it. Usually, we opt the minimum and maximum distances of 10 and 500 km, respectively.

Thus, one can use the long-term estimates of the USLE coefficients to characterize seismic hazard in a rather traditional terms of maximum expected magnitude and/or macro-seismic intensity, peak ground acceleration (PGA), etc. It should be noted that at a finer scale of seismic hazard determination, the USLE approach may help improving the neo-deterministic procedure (Panza et al. 2001, 2012) that supplies realistic time histories of strong ground motions, which allows to retrieve peak values for ground displacement, velocity, and design acceleration based on earthquake scenarios (e.g., Parvez et al. 2011; Paskaleva et al. 2011) and to address some issues largely neglected in traditional hazard analysis (i.e., local crustal properties, soils) by making use of all the available empirical data on the Earth's structure.

In assessment of seismic risks, we may face many different risk estimates even if the same object of risk is considered. Specifically, it may result from the different laws of convolution, as well as from different kinds of vulnerability of an object of risk under specific environments and conditions. Both conceptual issues must be resolved in a multidisciplinary problem-oriented research performed by specialists in the fields of hazard, objects of risk, and object vulnerability. Following (Parvez et al. 2014), to illustrate this general concept, we perform the oversimplified convolution of seismic hazard assessment map $H(x)$ with the population and its vulnerability $R(x) = H(x) \cdot \int P \cdot f(P)$, where $\int P$ is the integral of the population density over the cell x , i.e., the number of individuals within the area of the cell x , and $f(P)$ is individual vulnerability as a function of density distribution P . In application, we differentiate individual vulnerability in proportion to some power of the population density at a given site, which appears to be admissible due to specifics of man-made environment

inflicted in the areas of high concentration of individuals, e.g., the number of floors in typical residential building changes with population density. Risk estimates of this kind are given in Parvez et al. (2014).

3 Data

As the input of our pilot application to the territory of Greater Caucasus and Crimea, we used the following seismic and population data.

3.1 Seismic data

Seismicity of Greater Caucasus region is considered within $40^\circ\text{--}46^\circ\text{N}$ and $36^\circ\text{--}51.5^\circ\text{E}$. The regional catalogue is compiled using the annual periodicals *Earthquakes in Northeastern Asia (1998–2008)* and *Earthquakes in Russia (2004–2014)*. The regional catalogue is sufficiently complete in reporting earthquakes of energy class $K = 10.5$ or above (officially adopted in the Soviet Union), which range corresponds to magnitude $M = 3.6$ or larger (Fig. 1) and provides the sample of 4941 earthquakes (with depth above 70 km).

Seismicity of Crimea Peninsular region is considered within $44^\circ\text{--}46.5^\circ\text{N}$ and $32^\circ\text{--}37^\circ\text{E}$. Regretfully, the data from the recent abovementioned sources appear incomplete and, perhaps, irregular. Therefore, for the purposes of this study, we have used the Composite regional catalogue of Crimea compiled by Tatyana Rautian and Vitaly Ivanovich Khalturin using a series of yearbooks *Earthquakes in USSR in 1962–1991* published by Nauka Publishers in 1964–1997 (https://earthquake.usgs.gov/data/russia_seismicity/download/Crimea.ZIP). The earthquake hypocenters' data in 1962–1990 appears reasonably complete at the energy class $K > 7$, i.e., above magnitude $M = 1.7$ (Fig. 2), which sample size is 388 events.

3.2 Population data

The population data are taken from Gridded Population of the World (2005) that is a raster data product compiled at the Center for International Earth Science Information Network (CIESIN), Columbia University and Centro Internacional de Agricultura Tropical (CIAT). This population density distribution maps of the two regions based on the GPWv3 estimate for 2015 are given in Fig. 3. In addition to the distributed model data

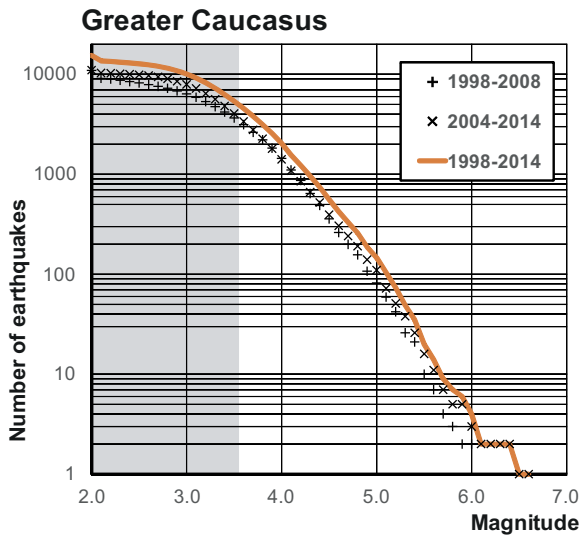


Fig. 1 Cumulative frequency-magnitude plot: Greater Caucasus, 1998–2014. The range of incomplete data is shaded in gray

for the territory, we use the available census data from Federal State Statistics Service (2016) to characterize seismic risks for the cities with population above 100,000 inhabitants in the regions of Greater Caucasus and Crimea. As demonstrated by Parvez et al. (2018), using actual census data on population of municipalities could be critical for realistic estimations of the expected risks.

3.3 Morphostructural nodes

The question where catastrophic earthquakes can happen is highly important for knowledgeable seismic hazard and risk assessment. A simple answer that large earthquakes can happen only in places where smaller magnitude quakes were registered in the past is not always correct as confirmed by seismological practice, which has many case histories of “surprises.” In our study, we expand the answer to the sites, which did not yet explicitly show up as earthquake-prone and consider the intersections of morphostructural lineaments of Crimea and Greater Caucasus (denoted as “nodes” below) as the suitable network of grid points for an USLE application. The principles of Morphostructural Zoning (MSZ), its formalization, and performance in recognition of the areas prone to large earthquakes in advance of their occurrence are described in Gorshkov et al. (2003) and Soloviev et al. (2014). The MSZ map of Greater Caucasus (Fig. 4) resulted from

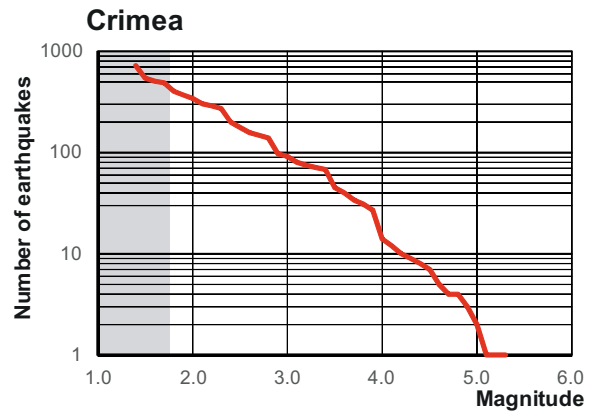


Fig. 2 Cumulative frequency-magnitude plot: Crimea, 1962–1990. The range of incomplete data is shaded in gray

field investigations by E.Ia. Rantsman, A.I. Gorshkov, and M.P. Zhidkov in the period from 1979 to 1984 (Gorshkov et al. 1986) and had been tested by seismic evidence after the first publication on several occasions (Soloviev et al. 2014). Specifically, all 13 earthquakes of magnitude 5 or larger in Greater Caucasus, 1988–2014, occurred in less than 25 km from the M5.0-prone nodes; nine of them from the areas where such earthquakes were not registered before 1988. The MSZ map of Crimea (Fig. 5) is compiled recently by A.I. Gorshkov (Gorshkov and Soloviev 2016) based on the same principles and, presumably, with the same accuracy. Thus, in the following application of the USLE-based approach, we consider 107 and 38 intersections of the MSZ lineaments in Greater Caucasus and Crimea, respectively.

4 Application of the SCE algorithm

In each of the two regions, the SCE algorithm was applied to the sample of earthquakes defined in Section 3.1 considered within the hierarchy of square boxes with linear size of 2° , 1° , $1/2^\circ$, and $1/4^\circ$ centered at each of the 145 nodes of the MSZ maps.

4.1 Greater Caucasus

Reliable estimates of coefficients A , B , and C were obtained for each of the 102 out of 107 nodes of Greater Caucasus, for which the number of earthquakes recorded in 1998–2014 is sufficient for application of the SCE algorithm. Figure 6 shows the maps of the estimates of

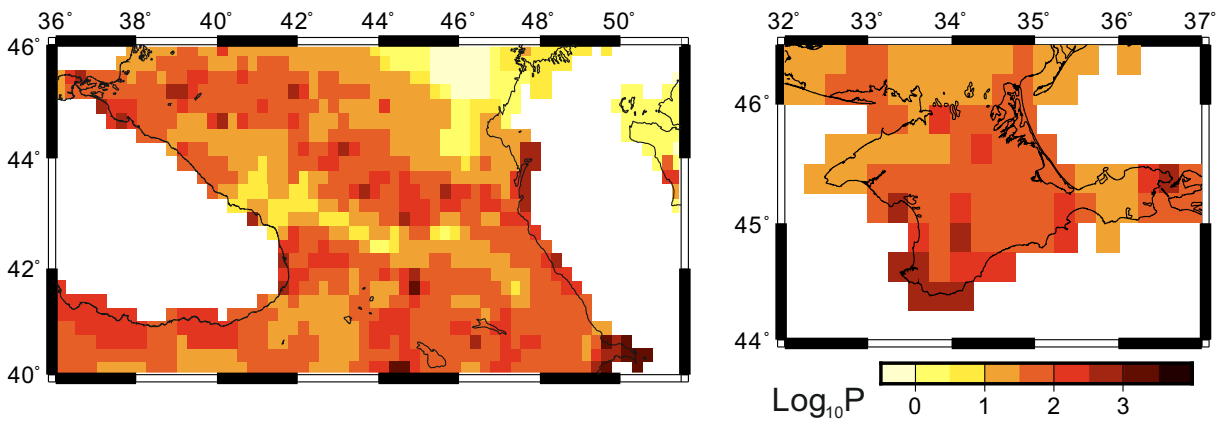


Fig. 3 The population density P (in ind/km²): The GPWv3 estimate for the year 2015

coefficients A , B , and C together with the squared sum of their standard errors σ_A , σ_B , and σ_C . The densities of their distributions are given in Fig. 7. The error of determination of the USLE coefficients at all 102 nodes does not exceed 0.05, which confirms rather high quality of the mapped values for the entire territory of Greater Caucasus.

The distribution of the level of seismic activity (coefficient A) has four characteristic maxima, of which the two largest at A about 0 and 0.3 correspond to the expectation of about one and two earthquakes with $M=5.0$ in a year. Most of the positive A s are located in Dagestan. The mean values of A , in which the

earthquake rate of occurrence is three times smaller, are spread in the central and eastern regions of Greater Caucasus. The other seismically active regions here are characterized by even lower level of recurrence of moderate earthquakes.

Most of the B values, which characterize the slope of the frequency-magnitude graph, vary from 0.7 to 1.4 with two pronounced peaks at 0.8 and 1.2 (a 2% peak at about 0.5 is related to the nodes in the south-eastern part of Greater Caucasus where the catalogue is apparently incomplete). The estimates of B below 0.6 to the west of 40°E appear to be outlier-related local incompleteness of the catalogue due to deficiency of seismographic

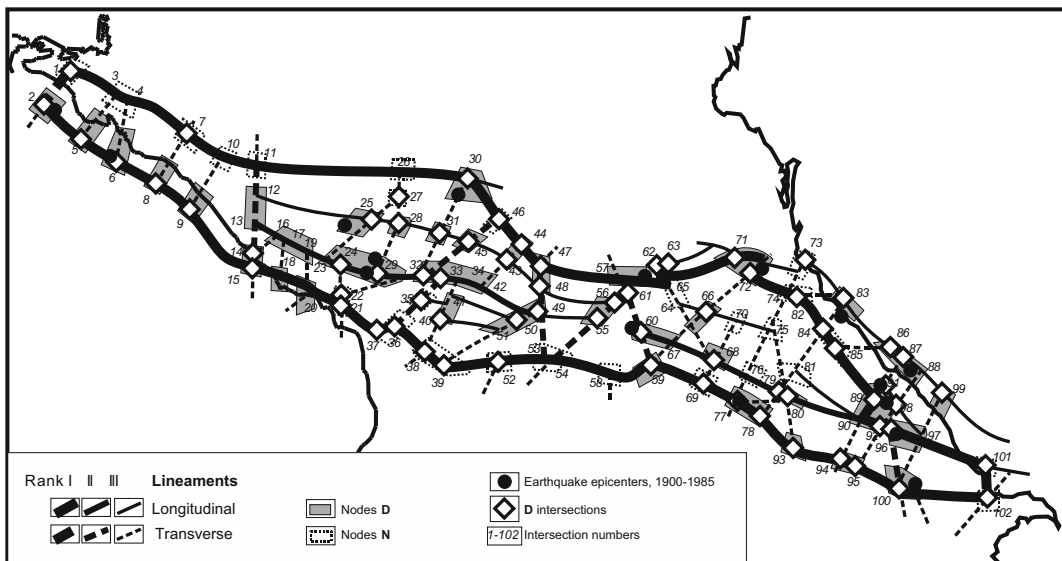


Fig. 4 The MSZ map of Greater Caucasus (after Gorshkov et al., 2003)

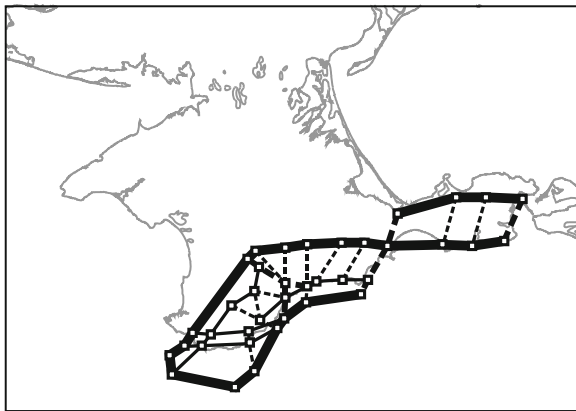


Fig. 5 The MSZ map of the Crimea Peninsula (after Gorshkov and Soloviev 2016)

stations, which network is gradually improving from two stations before 2003 to eight in 2013 (Table 1.5 in Gabsatarova et al. 2015).

The fractal dimension of distributed epicenters C varies from below 0.6 to 1.5 with the two clear peaks about 1.1 and 1.4. The first generally corresponds to the linear extension of dominant morphostructures of

Greater Caucasus, and the second—to the most fractured areas in the south-east of it, where the values of $C > 1.2$, i.e., the seismically active regions of Dagestan, Chechnya, and Karachay-Cherkessia.

4.2 Crimea Peninsula

Reliable estimates of coefficients A , B , and C were obtained for each of the 38 nodes of Crimea, where earthquake catalogue, 1962–1990 appears sufficient for application of the SCE algorithm. Figures 8 and 9 for Crimea are analogous to Figs. 6 and 7. The error of determination of the A , B , and C coefficients at all 38 nodes does not exceed 0.02, which is indicative of a higher quality of the mapped values in Crimea than in Greater Caucasus and, apparently, related to much longer period covered by the catalogue, i.e., 28 and 17 years, respectively.

The distribution of coefficient A ranges from -2 to -1.4 , which corresponds to the expectation of one earthquake with $M = 5.0$ in 100 and 25 years, respectively, i.e., much lower rate of moderate earthquakes than in

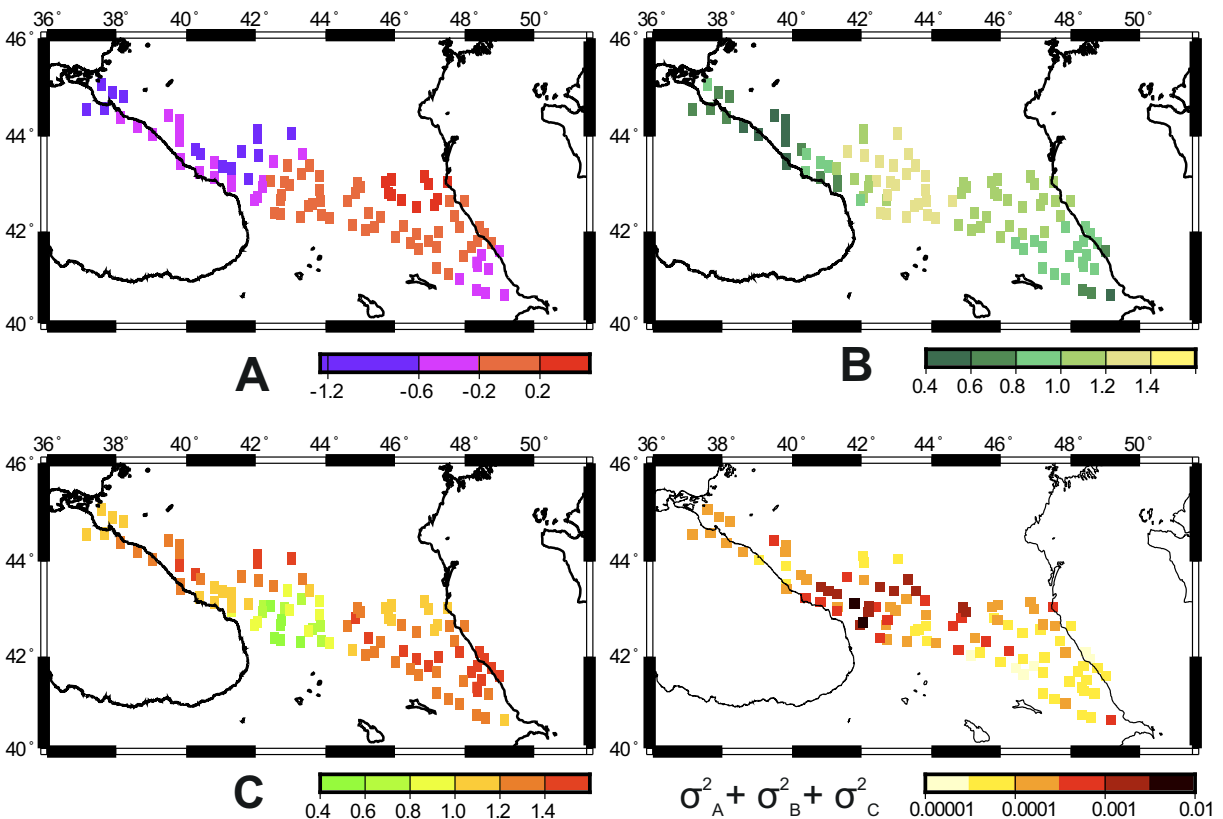


Fig. 6 The maps of the A , B , C estimates and of the squared sum of their errors at the MSZ nodes of Greater Caucasus

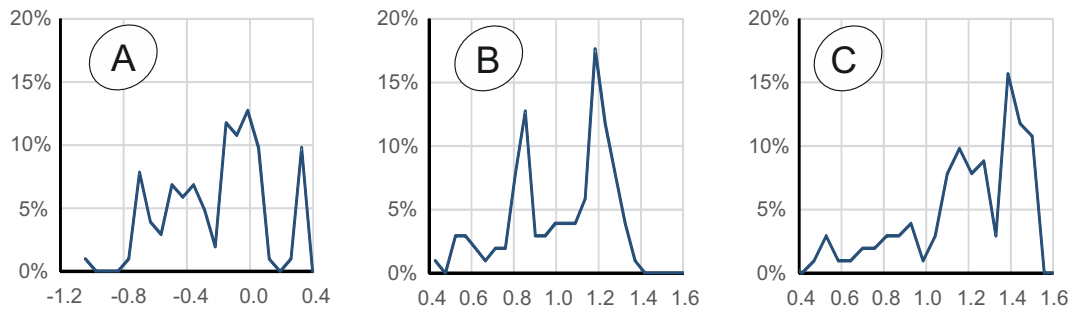


Fig. 7 The density distributions of the *A*, *B*, *C* estimates at the MSZ nodes of Greater Caucasus

Greater Caucasus. The values of coefficient *B* vary in a narrow range from below 0.5 to 0.9 with a peak at 0.7. The values of coefficient *C* are mainly in range from 0.8 to 1.0 with a high peak at about 0.9, which reminds the classical 1D Cantor “dust” with $P = 0.9$ and $df = \log(P)/\log(2) \approx 0.85$, a possible indication of a linear fault zone in decline of tectonic activity.

5 Hazard and risk determination

The USLE coefficients determined at the nodes of morphostructures were used to determine the distribution of the magnitude of the MCE events in the two regions (as described in step 6 of Section 2). As an exception, we used the pattern recognition results from Gvishiani et al. (1988); Gorshkov et al. (2003); and Soloviev et al. (2013) for the eight nodes with *B* below 0.6 to the west of 40°E. The resulting maps of *M*_{max} given in Fig. 10 disclose significant difference of seismic hazard expectations in Greater Caucasus, where *M*_{max} above 6.5 is widespread along the entire mountain range, and Crimea, where the exceedance of such a level appears to be rather unlikely. The seismic hazard, in terms of PGA with 10% of exceedance in 50 years, for the entire territories of the two regions is given in Fig. 11; according to computations based on the distribution of *M*_{max}, the ground shaking in Greater Caucasus may exceed the level of 1g, while in Crimea, it is hardly possible, except for the south-eastern part of the peninsula.

As an illustration of the complexity of seismic risk assessment, we calculated (step 7, Section 2) and plotted the maps of $R_{ii}(x) = H(x) \cdot x^P \cdot P$ and $R_{iv}(x) = H(x) \cdot x^P \cdot P^3$ where individual vulnerability is proportional to the 1st and the 3rd power of population density, correspondingly (Fig. 12). For each of the two maps, the

risk is given in arbitrary units proportional to the maximum value defined as 1000, so that the risk estimates provided in terms of a non-dimensional index, ranging from 0 to 1000. The color of a cell corresponds to the

Table 1 Seismic hazard and risk at major cities of the two regions

City	Population	S (km ²)	PGA (g)	<i>R</i> _{ii} (au)	<i>R</i> _{iv} (au)
Krasnodar	853,848	339	0.41	746	436
Makhachkala	587,876	468	1.19	739	108
Stavropol	429,571	172	0.08	73	42
Sevastopol*	416,263	1080	0.43	58	1
Sochi	401,291	177	0.81	618	293
Simferopol	336,460	107	0.54	477	432
Vladikavkaz	307,478	291	1.34	368	38
Grozny	287,410	324	1.93	415	30
Novorossiysk	266,977	81	1.35	1000	1000
Nalchik	239,040	67	0.81	585	687
Kerch	148,932	108	0.16	28	5
Pyatigorsk	145,448	97	0.43	78	16
Maykop	144,055	59	0.54	161	90
Khasavyurt	138,420	40	1.22	492	544
Kislovodsk	129,993	72	0.70	138	42
Cherkessk	123,128	70	0.62	113	32
Derbent	122,354	70	1.61	292	83
Nevinnomyssk	117,891	100	0.32	37	5
Nazran	113,288	80	1.15	155	29
Kaspiysk	110,080	33	1.14	353	364
Yevpatoriya	106,202	291	0.11	3	0.1
Essentuki	105,881	50	0.33	63	26
Yalta	78,452	18	0.46	132	225

Cities are given in descending order by population. The values of risk are given in arbitrary units proportional to the maximum of 1000. The top five values of parameters are given in italics. *Sevastopol, in the borders which include the city of Inkerman, town of Balaklava, Kacha village, and 39 settlements with the rural population (Federal State Statistics Service 2016)

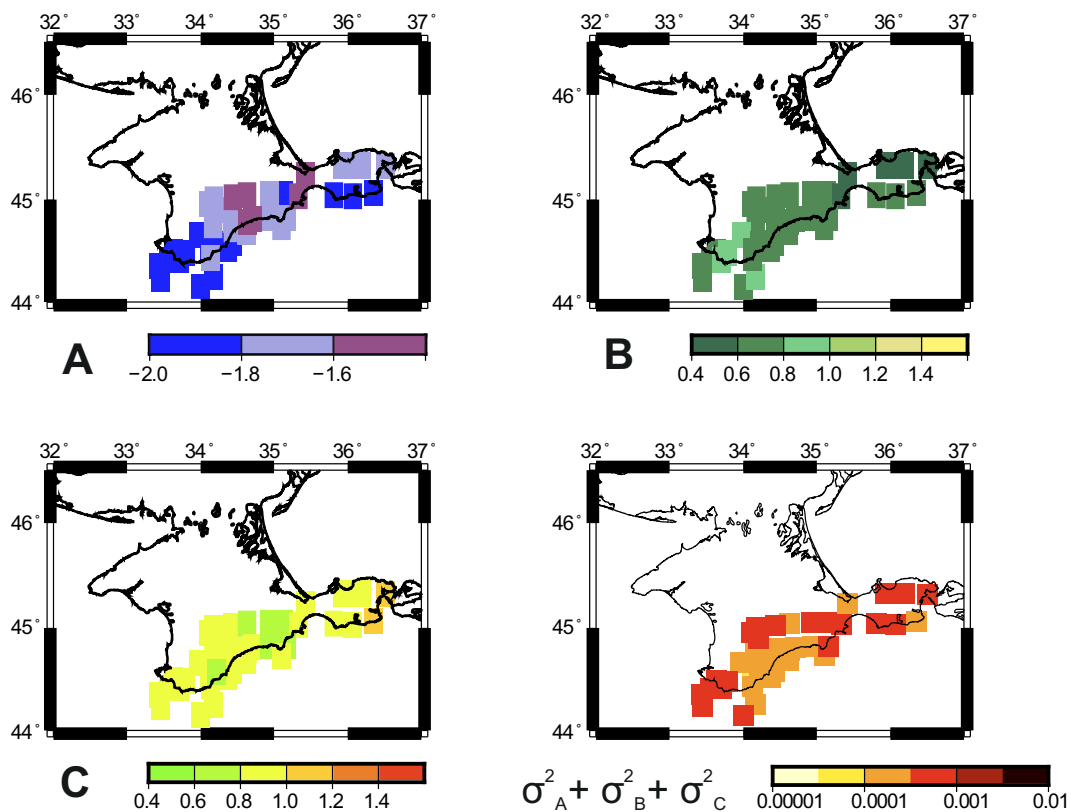


Fig. 8 The maps of the *A*, *B*, *C* estimates and of the squared sum of their errors at the MSZ nodes of Crimea

decimal logarithmic scale in range from 1000 to 0.01. Not a surprise that the maximum risk for population is concentrated at the urban agglomerations and drops dramatically when moving to the rural districts of the two regions.

Table 1 summarizes the results of seismic hazard and risk estimates for the 18 cities with population above 100,000 inhabitants affected by earthquakes of Greater Caucasus and the five largest cities of Crimea. The top five values of Population, city area *S*, PGA, R_{ii} , and R_{iv}

are highlighted disclosing the complex combinations of possibilities. For example, the city of Sevastopol and its agglomeration from the top five in population is among the lowest of the 23 cities in respect to the risk estimates due to the largest area and moderate seismic hazard; the capital of Chechen Republic, Grozny, although of the highest expected ground shaking, is on the 8th and 15th place in regard to R_{ii} and R_{iv} ; the city of Novorossiysk gets the highest risk estimates due to the 3rd largest PGA and its area just below the median of *S*. The matrix

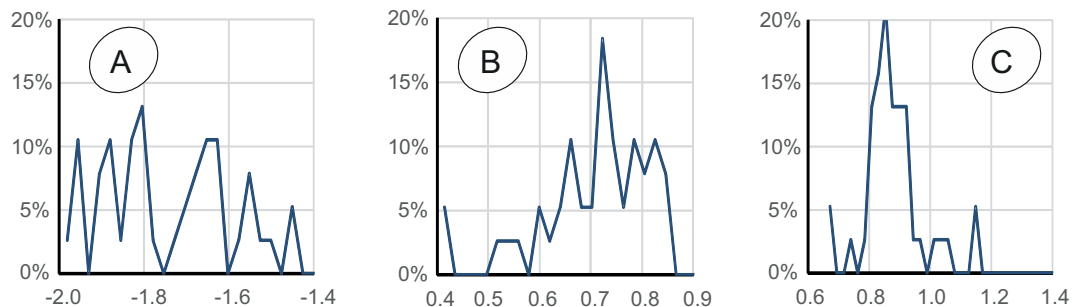


Fig. 9 The density distributions of the *A*, *B*, *C* estimates at the MSZ nodes of Crimea

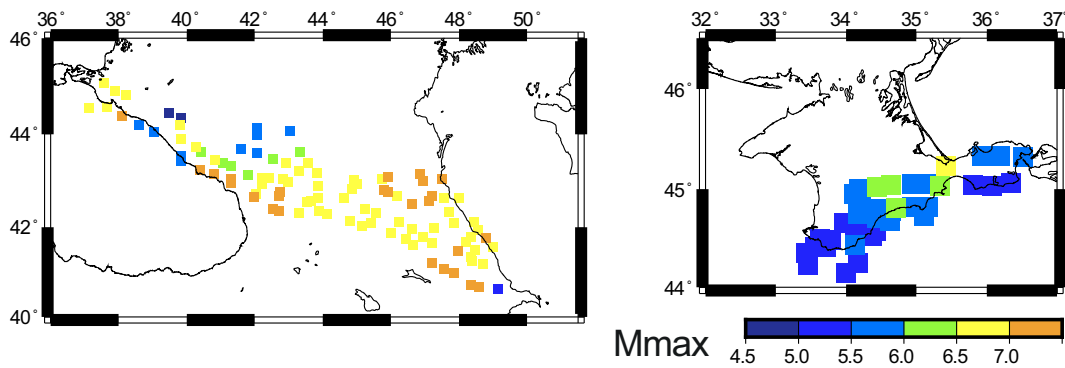


Fig. 10 The maps of the USLE-based maximal magnitude, M_{max} , at the MSZ nodes of Greater Caucasus and Crimea

of correlation coefficients (Table 2) between the city parameters with or without the Sevastopol agglomeration from Table 1 shows up quite expected dependence of the risk estimates on the number of citizens and seismic hazard, while their anti-correlation with the city area.

Let us emphasize that the hazard and risk estimates for the two regions under study are presented here for academic methodological purposes highlighting the general problem-oriented approach based on USLE. Evidently, our estimates do not use more adequate though complicated procedures of convolutions of seismic hazard, objects of risks, and their vulnerability. The estimations addressing more realistic and practical kinds of seismic risks should involve regional experts in earthquake engineering, social sciences, and economics.

6 Discussion and conclusions

The results of our pilot investigation of seismic hazard and risks of Greater Caucasus and Crimea disclose their

natural mid-term and spatial variability (Nekrasova and Kossobokov 2016). The maps of seismic hazard in terms of PGA with 10% rate of exceedance in 50 years for the two adjacent regions are dramatically different (Figs. 10 and 11). Moreover, the accuracy of this parameter determination differs from place to place. We should emphasize once again that, despite an apparent similarity with the PSHA estimation, the proposed maps based on USLE do not involve assumptions about temporal probability of earthquake occurrence. This is one of the basic differences between PSHA and neo-deterministic USLE-based approach, in general, as well as essentially deterministic USLE-based realization presented in this study. The basic seismic hazard estimates determined by means of the neo-deterministic seismic hazard assessment (NDSHA) is substantially different from popular deterministic seismic hazard assessment (DSHA): the in-detail discussion of the NDSHA enhancement and other alternatives to probabilistic seismic hazard analysis (PSHA) can be found in Panza et al. (2011, 2014). In particular, the existing seismic history is short; getting, experimentally, reasonable confidence

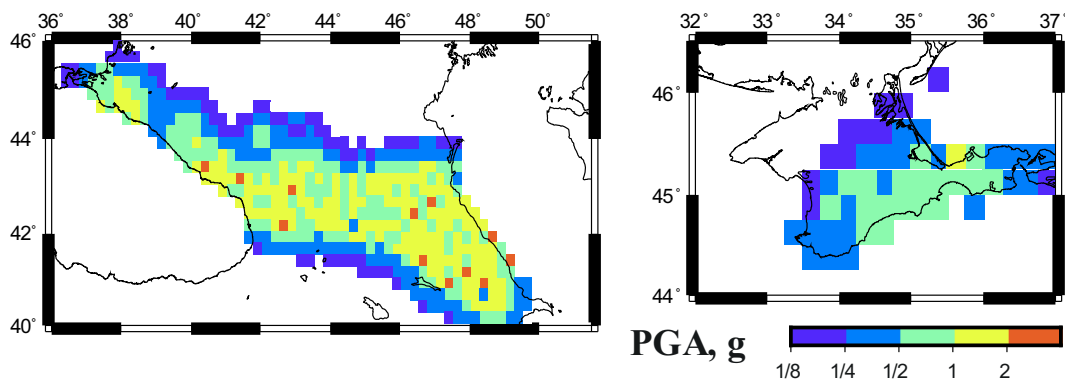


Fig. 11 The seismic hazard maps of Greater Caucasus and Crimea based on the USLE approach in terms of expected peak ground acceleration, PGA, with 10% chance of exceedance in 50 years

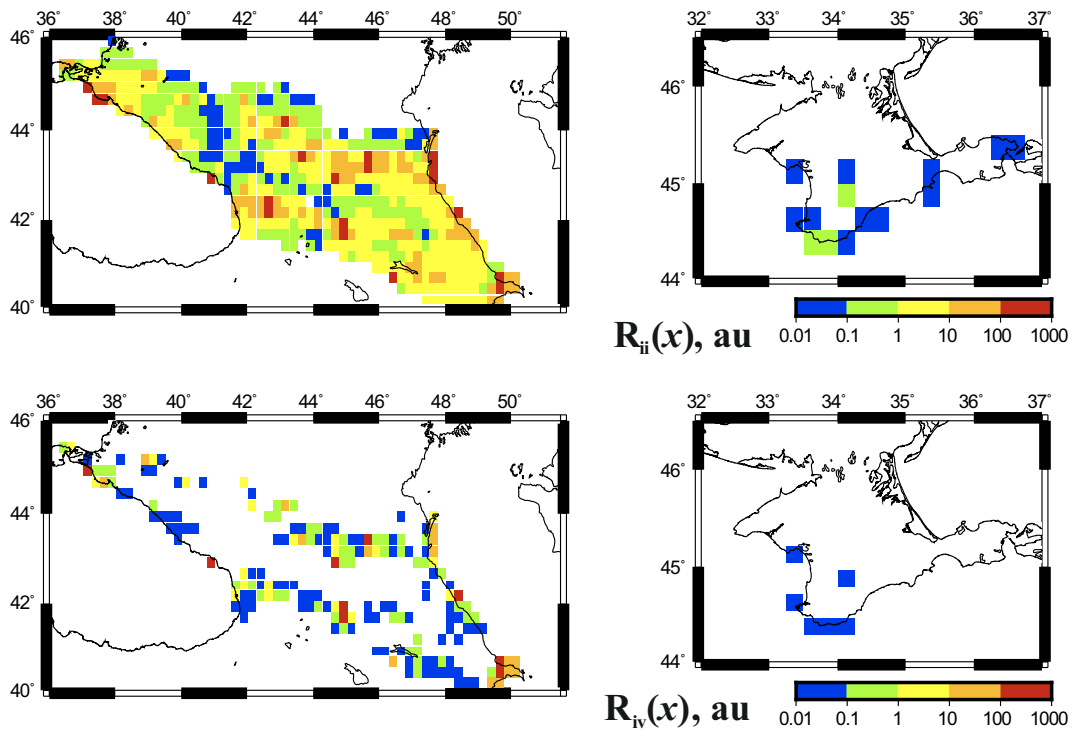


Fig. 12 The seismic risk maps of Greater Caucasus and Crimea based on the USLE approach in terms of $R_{ii}(x) = H(x) \cdot xP \cdot P$ (top row) and $R_{iv}(x) = H(x) \cdot xP \cdot P^3$ (bottom row)

limits on an objective estimate of recurrence rate of an earthquake on a local, or even on a regional scale, requires a geologic span of time above 10,000 years, which is unreachable for instrumental, or even historical, seismology (see, e.g., Beauval et al. 2008). Therefore, seismic hazard estimates may not rely exclusively on earthquake instrumental data and require the neo-deterministic assessment based on a solid geological evidence and pattern recognition of earthquake-prone areas (Panza et al. 2001, 2011, 2012, 2014; Peresan and Panza 2012; Peresan et al. 2011). Nevertheless, just the

5 out of 344 moderate ($M \geq 5.0$, 550 BC–present) earthquakes in Greater Caucasus and 7 out of 22 of such earthquakes in Crimea might indicate the sites where the seismic hazard is underestimated in our analysis presented in terms of M_{max} at MSZ nodes (Fig. 10). All these “surprises” are listed in Table 3, and all of them are from the seismic history of the regions when determination of earthquake parameters is very uncertain (Kondorskaya et al. 1982); enough mentioning of the deadliest 1668 Shemakhi earthquake, which magnitude could be as low as 7.0 with a possibility of at least two

Table 2 Correlations of city parameters

	Population	S (km ²)	PGA (g)	R_{ii} (au)	R_{iv} (au)
Population	100%	53.0%	− 1.2%	56.3%	19.8%
S (km ²)	71.5%	100%	− 4.1%	0.7%	− 23.3%
PGA (g)	1.7%	16.2%	100%	52.9%	26.3%
R_{ii} (au)	62.4%	34.1%	51.6%	100%	79.4%
R_{iv} (au)	23.6%	− 18.7%	24.6%	78.8%	100%

The italic and bold values are estimates based on data for the cities in Table 1 with and without the Sevastopol agglomeration, correspondingly

Table 3 The earthquakes, 550 BC–2016, which magnitude M is larger than M_{\max} at the distance of $1/2^\circ$ or less

Year	Month	Day	Lat	Lon	$M \pm \text{err}M$	M_{\max}	$\Delta M = M - M_{\max}$
Greater Caucasus							
1100	na	na	43.1	42.4	7.1 ± 0.7	7.0	0.1
1275	4	14	41.9	44.6	6.7 ± 0.5	6.6	0.1
1668	1	14	41.0	48.0	7.8 ± 0.5	7.1	0.7
1742	8	5	42.1	45.2	6.7 ± 0.5	6.6	0.1
1905	10	21	43.3	41.7	6.4 ± 0.3	6.1	0.3
Crimea							
63 BC	10	na	45.6	36.2	6.4 ± 0.7	5.8	0.6
275	na	na	45.2	36.5	6.4 ± 1.0	5.7	0.7
1450	na	na	44.3	34.3	6.5 ± 1.0	5.9	0.6
1793	12	8	44.8	33.2	5.5 ± 1.0	5.3	0.2
1902	1	8	44.6	35.8	5.5 ± 0.5	5.4	0.1
1927	6	26	44.5	34.3	6.0 ± 0.1	5.9	0.1
1927	9	11	44.3	34.3	6.8 ± 0.1	5.9	0.9

alternative dates either on February 17, 1667 or January 04, 1668 (Utsu 2002). The reported magnitude determination error (above 0.5 attributed to 9 out of these 12 earthquakes in Kondorskaya et al. (1982)) permits limiting the scores of “surprises” to the two cases of 1668 Shemakhi and September 11, 1927 Yalta earthquakes and conclude quite acceptable the level of underestimation of the obtained seismic hazard maps of Greater Caucasus and Crimea.

On the other hand, the hazard maps in Fig. 11 are much more cautious and site-specific than the one of the Global Seismic Hazard Assessment Program (Giardini et al. 1999; Giardini et al., 2003). In particular, the GSHAP PGA values are in contradiction to the historical evidence of 21 and 6 “surprises” of the GSHAP hazard maps for Greater Caucasus and Crimea, respectively. The scores to be compared with the only 6 “surprises” out of 366 historical trials of the hazard maps of the regions in Fig. 11. All this favors the neo-deterministic USLE-based approach to the problem of assessing seismic hazard and risks showing that its hazard maps perform more reliably than those of PSHA.

Our study attempts to contribute an urgent revision of the probabilistic seismic hazard maps by an improvement of background methodologies and implementation in assessment of seismic hazard and risks. Evidently, it does not take into consideration economic and social factors of risk assessment, neither account for the role of site effect due to topography and soils, nor make use of

an earthquake rupture size for the large and/or complex seismic events. These essential considerations should be addressed in the future practical estimations and mappings.

Funding information The study was supported by the Russian Science Foundation (Grant No. 15-17-30020).

References

- Bak P, Christensen K, Danon L, Scanlon T (2002) Unified scaling law for earthquakes. *Phys Rev Lett* 88:178501–178504
- Beauval C, Hainzl S, Scherbaum F (2006) The impact of the spatial uniform distribution of seismicity on probabilistic seismic-hazard estimation. *Bull Seismol Soc Am* 96(6):2465–2471. <https://doi.org/10.1785/0120060073>
- Beauval C, Bard P-Y, Hainzl S, Guéguen P (2008) Can strong-motion observations be used to constrain probabilistic seismic-hazard estimates? *Bull Seismol Soc Am* 98(2):509–520. <https://doi.org/10.1785/0120070006>
- Christensen K, Danon L, Scanlon T, Bak P (2002) Unified scaling law for earthquakes. *Proc Natl Acad Sci* 99(suppl 1):2509–2513
- Davis C, Keilis-Borok V, Kossobokov V, Soloviev A (2012) Advance prediction of the March 11, 2011 Great East Japan earthquake: a missed opportunity for disaster preparedness. *Int J Disaster Risk Reduct* 1:17–32. <https://doi.org/10.1016/j.ijdrr.2012.03.001>
- Federal State Statistics Service, 2016. The population of the Russian Federation for municipalities on January 1, 2016. FSSS: Moscow, Russian Federation. <http://www.gks.ru/>

- free_doc/doc_2016/bul_dr/mun_obr2016.rar (assessed 19.09.2016)
- Gabsatarova, I.P., Daniyalov, M.G., Mekhryushev, D.Yu., Pogoda, E.V., Yatskov, A.Yu., 2015. Northern Caucasus, in: Malovichko, A.A. (Ed.), The earthquakes of Russia in 2013. GS RAS, Obninsk, 16–21
- Giardini D, Grünthal G, Shedlock K, Zhang P (1999) The GSHAP Global Seismic Hazard Map. *Ann Geofis* 42(6):1225–1228
- Giardini D, Grünthal G, Shedlock K, Zhang P (2003) The GSHAP Global Seismic Hazard Map. In: Lee WHK, Kanamori H, Jennings P, Kisslinger C (eds) *International handbook of earthquake and engineering seismology, International Geophysics Series 81 B*. Academic Press, Amsterdam, pp 1233–1239
- Gorshkov, A., Soloviev, A., 2016. Crimea: morphostructural zoning and seismogenic nodes. 35th General Assembly of the European Seismological Commission, Abstract ESC2016–688. <http://meetingorganizer.copernicus.org/ESC2016/ESC2016-688.pdf> (accessed 19.10.2016)
- Gorshkov A, Gvishiani A, Kossobokov V, Rantsman E (1986) Morphostructures and places of earthquakes in the Greater Caucasus. *Izvestia Acad. Sci. SSSR: Phys. Earth* 9:24–35 (in Russian)
- Gorshkov A, Kossobokov V, Soloviev A (2003) Chapter 6. Recognition of earthquake-prone areas. In: Keilis-Borok VI, Soloviev AA (eds) *Nonlinear dynamics of the lithosphere and earthquake prediction*. Springer, Heidelberg, pp 239–310
- Gridded Population of the World, Version 3 (GPWv3), 2005. Palisades, NY: Socioeconomic Data and Applications Center (SEDAC), Columbia University, <http://sedac.ciesin.columbia.edu/gpw> (accessed 05.07.2016)
- Gvishiani A, Gorshkov A, Rantsman E, Cisternas A, Soloviev A (1988) Identification of earthquake-prone-areas in the regions of moderate seismicity. *Nauka, Moscow*, p 175 (in Russian)
- Kondorskaya, N.V., Shebalin, N.V., Khrometskaya, Ya.A., Gvishiani, A.D., 1982. New catalog of strong earthquakes in the U.S.S.R. from ancient times through 1977. World Data Center A for Solid Earth Geophysics, Report SE-31, 609 pp.
- Kossobokov, V.G., 2005. Earthquake prediction: principles, implementation, perspectives, in: *Earthquake prediction and geodynamic processes. Part 1 (computational seismology, issue 36)*, Moscow, GEOS, 179 pp. (in Russian)
- Kossobokov, V.G., Mazhkenov, S.A., 1994. On similarity in the spatial distribution of seismicity, in: Chowdhury, D.K. (Ed.) *Computational Seismology and Geodynamics*, 1 AGU, The Union, Washington DC, 6–15
- Kossobokov V, Nekrasova A (2012) Global seismic hazard assessment program maps are erroneous. *Seismic Instruments* 48(2): 162–170. <https://doi.org/10.3103/S0747923912020065>
- Kossobokov V, Peresan A, Panza GF (2015) Reality check: seismic hazard models you can trust. *Eos* 96(13):9–11
- Nekrasova, A.K., 2008. Unified Scaling Law for Earthquakes: implications for seismic active word zones. (PhD. Thesis), M.V. Lomonosov Moscow State University, Moscow, 136 pp. (in Russian)
- Nekrasova AK, Kosobokov VG (2005) Temporal variations in the parameters of the Unified Scaling Law for Earthquakes in the eastern part of Honshu Island (Japan). *Dokl Earth Sci* 405: 1352–1356
- Nekrasova AK, Kosobokov VG (2006) Unified scaling law for earthquakes in the Lake Baikal region. *Dokl Earth Sci* 407A(3):484–485
- Nekrasova AK, Kosobokov VG (2016) Unified Scaling Law for Earthquakes in Crimea and Northern Caucasus. *Doklady Earth Sci*, 2016 470(2):1056–1058. <https://doi.org/10.1134/S1028334X16100032>
- Nekrasova A, Kossobokov V (2002) Generalizing the Gutenberg–Richter scaling law. *EOS Trans AGU* 83(47):NG62B–N0958
- Nekrasova A, Kossobokov V, Perezan A, Aoudia A, Panza GF (2011) A multiscale application of the Unified Scaling Law for Earthquakes in the Central Mediterranean area and Alpine region. *Pure Appl Geophys* 168:297–327. <https://doi.org/10.1007/s00024-010-0163-4>
- Nekrasova, A., Peresan, A., Kossobokov, V.G., Panza, G.F., 2014. Chapter 7: a new probabilistic shift away from seismic hazard reality in Italy?, in: Aneva, B., Kouteva-Guentcheva, M. (Eds.), *Nonlinear Mathematical Physics and Natural Hazards, Springer Proceedings in Physics*, 163, 83–103. https://doi.org/10.1007/978-3-319-14328-6_7
- Nekrasova A, Kossobokov V, Parvez IA, Tao X (2015) Seismic hazard and risk assessment based on the unified scaling law for earthquakes. *Acta Geod Geophys* 50(1):21–37. <https://doi.org/10.1007/s40328-014-0082-4>
- Panza GF, Romanelli F, Vaccari F (2001) Seismic wave propagation in laterally heterogeneous anelastic media: theory and applications to seismic zonation. *Adv Geophys* 43:1–95
- Panza, G., Irikura, K., Kouteva-Guentcheva, M., Peresan, A., Wang, Z., Saragoni, R. (Eds.), 2011. Advanced seismic hazard assessment, *pure Appl. Geophys.* 168(1–4), 752 pp.
- Panza, G.F., La Mura, C., Peresan, A., Romanelli, F., Vaccari, F., 2012. Seismic hazard scenarios as preventive tools for a disaster resilient society, in: Dmowska, R. (Ed.), *Adv. Geophys.*, Elsevier, London, 93–165
- Panza GF, Kossobokov V, Peresan A, Nekrasova A (2014) Chapter 12. Why are the standard probabilistic methods of estimating seismic hazard and risks too often wrong? In: Wyss M, Shroder J (eds) *Earthquake hazard, risk, and disasters*. Elsevier, London, pp 309–357
- Parvez IA, Vaccari F, Panza GF (2003) A deterministic seismic hazard map of India and adjacent areas. *Geophys J Internat* 155:489–508. <https://doi.org/10.1046/j.1365-246X.2003.02052.x>
- Parvez IA, Romanelli F, Panza GF (2011) Long period ground motion at bedrock level in Delhi city from Himalayan earthquake scenarios. *Pure Appl Geophys* 168:409–477. <https://doi.org/10.1007/s00024-010-0162-5>
- Parvez IA, Nekrasova A, Kossobokov V (2014) Estimation of seismic hazard and risks for the Himalayas and surrounding regions based on Unified Scaling Law for Earthquakes. *Nat Hazards* 71(1):549–562. <https://doi.org/10.1007/s11069-013-0926-1>
- Parvez IA, Nekrasova A, Kossobokov VG (2018) Seismic hazard and risk assessment based on Unified Scaling Law for Earthquakes: thirteen principal agglomerations of India. *Nat Hazards*. <https://doi.org/10.1007/s11069-018-3261-8>
- Paskaleva I, Kouteva-Guentcheva M, Vaccari F, Panza GF (2011) Some contributions of the neo-deterministic seismic hazard assessment approach to earthquake risk assessment for the city of Sofia. *Pure Appl Geophys* 168:521–541. <https://doi.org/10.1007/s00024-010-0127-8>
- Peresan A, Panza GF (2012) Improving earthquake hazard assessment in Italy: an alternative to “Texas sharpshooting”. *EOS*

- Trans Am Geophys Union 93(51):538–539. <https://doi.org/10.1029/2012EO510009>
- Peresan A, Zuccolo E, Vaccari F, Gorshkov A, Panza GF (2011) Neo-deterministic seismic hazard and pattern recognition techniques: time-dependent scenarios for North-Eastern Italy. *Pure Appl Geophys* 168(3):583–607. <https://doi.org/10.1007/s00024-010-0166-1>
- Soloviev AA, Novikova OV, Gorshkov AI, Piotrovskaya EP (2013) Recognition of potential sources of strong earthquakes in the Caucasus region using GIS technologies. *Doklady Earth Sc* 450:658–660. <https://doi.org/10.1134/S1028334X13060159>
- Soloviev AA, Gvishiani AD, Gorshkov AI, Dobrovolsky MN, Novikova OV (2014) Recognition of earthquake prone areas: methodology and analysis of the results. *Izvestiya, Physics of the Solid Earth* 50(2):151–168. <https://doi.org/10.1134/S1069351314020116>
- Utsu, T., 2002. A list of deadly earthquakes in the world: 1500–2000, in: Lee, W.H.K., Kanamori, H., Jennings, P.C., Kisslinger, C. (Eds.), *International handbook of earthquake & engineering seismology part A*, Academic Press, San Diego, 691–717
- Wyss M, Nekrasova A, Kossobokov V (2012) Errors in expected human losses due to incorrect seismic hazard estimates. *Nat Hazards* 62(3):927–935. <https://doi.org/10.1007/s11069-012-0125-5>